# On the properties of $Cu_2ZnSn(S,Se)_4$ thin films prepared by selenization of binary precursors using rapid thermal processing

M R Rajesh Menon[1], Samaneh Ranjbar[1], M G Sousa[1], P A Fernandes[1,2] and A F da Cunha[1]

[1]I3N-Departamento de Física, Universidade de Aveiro, Campus Universitário de Santiago, 3810-193 Aveiro, Portugal.

[2]Departamento de Física, Instituto Superior de Engenharia do Porto, Instituto Politécnico do Porto, Rua Dr António Bernardino de Almeida, 431, 4200-072 Porto, Portugal. E-mail: rajeshmenon@ua.pt

## Abstract

$Cu_2ZnSn(S,Se)_4$ thin films were grown on molybdenum coated glass substrates by selenization of stacked precursor layers of zinc, tin disulfide and copper sulfide. Selenization was performed using a rapid thermal processor at maximum temperatures in the range of 400 °C to 550 °C and at heating rates of 1 °C /s and 2 °C /s. The compositional, morphological and structural characterization of the films was carried out using energy dispersive x-ray spectroscopy, scanning electron microscopy, x-ray diffraction and Raman spectroscopy. X-ray diffrac- tion and Raman scattering analysis suggests the formation of $Cu_2ZnSn(S,Se)_4$ only at lower temperatures, whereas $Cu_2ZnSnSe_4$ was formed at higher tem- peratures regardless of the heating rate used. Compositional analysis revealed that the films were Zn-poor and Sn-rich. However, the samples approach a near stoichiometric composition due to the loss of tin at a selenization temperature and heating rate of 550 °C and 2 °C/s, respectively. Large grains with an average lateral dimension of 4.5 µm were observed for films prepared at these conditions which are very desirable for an absorber for solar cells.

**Keywords**: $Cu_2ZnSn(S,Se)_4$, kesterite, rapid thermal processing, selenization, thin film solar cell

## 1. Introduction

The search for an efficient and cost-effective absorber material for solar cells is always in the forefront of photovoltaic research. Several new materials are being investigated resulting in positive implications, but still, $Cu_2ZnSn(S,Se)_4$ (CZTSSe) remains a leading candidate at present due to its many attractive features such as the abundance and low-cost of its constituent elements and potential for higher conversion efficiencies [1]. The preparation of CZTSSe thin films usually follows a two-stage process which starts with the deposition of metallic or compound precursors and subsequent sulfurization/selenization at high temperatures. A variety of techniques were employed to deposit precursor films including physical vapor deposition [2–5], electro-deposition [6], using inks of nanoparticle precursors [7, 8] and using hydrazine-based pure solution approach [9]. The subsequent sulfurization/selenization process at high temperatures is crucial in promoting the grain growth and conversion of precursors to CZTSSe, and has significant impact on the properties of the films [10, 11]. However, it may happen that there can be loss of elements, especially zinc and tin, during this high temperature step and this leads to significant deviation in composition of the resulting films from that of the precursor [12–14]. Rapid thermal processing (RTP) is a superior technique compared to a conventional annealing system since it involves shorter times in attaining maximum annealing temperatures and hence minimizes the loss of volatile components in the precursor and decomposition of final product [15]. In this report we employed RTP to selenize precursor stack consisting of metallic zinc, tin disulfide and copper sulfide. The processing conditions were varied and its effects on the compositional, morphological and structural properties of the films were studied.

## 2. Experimental details

CZTSSe thin films were prepared by a two-step process, the first involving deposition of the precursor stack on Mo-coated glass substrate and the second involving its selenization in a rapid thermal processor. The precursors used were metallic zinc (Zn), tin disulfide ($SnS_2$) and copper sulfide (CuS). Zn was deposited using thermal evaporation of Zn pellets (99.999% purity) from a molybdenum crucible whereas an RF magnetron system consisting of compound targets was employed to deposit $SnS_2$ and CuS. The sequential deposition of the precursors was carried out in an Ar atmosphere, at an operating pressure of $4.0 \times 10^{-3}$ mbar. The process was repeated in

eight periods to prepare stacked layers of precursors in the order Zn/$SnS_2$/CuS. In order to selenize the precursors so as to form CZTSSe, about 1.5 μm thick layer of Se was deposited over the precursor stacks after which they were annealed in the RTP furnace using $N_2$ + 5% $H_2$ gas at a pressure of 1 atm. The precursors were annealed at maximum annealing temperatures of 400, 450, 500 and 550 °C for 2 min. Two different heating rates were tried viz. 1 °C/s and 2 °C/s. These heating rates were selected in order to take advantage of RTP. Unfortunately, higher heating rates above 2 °C/s resulted in the delamination of the underlying Mo layer from the substrate. All the samples were prepared from a similar precursor stack and the thickness of the selenized films were approximately 600 nm. The morphology and the composition of the films were investigated by scanning electron microscopy (SEM) and energy dispersive x-ray spectroscopy (EDS), using an SU-70 Hitachi combined with a Rontec EDS system, at an acceleration voltage of 25 kV. The structural analysis was done using x-ray diffraction (XRD) and Raman spectroscopy. XRD patterns were acquired using an XPert MPD Philips

diffractometer in the Bragg–Brentano configuration (θ–2θ), using the Cu-$K_\alpha$ line (λ = 1.5406 Å), with the generator settings, 40 mA and 45 kV. Raman measurements were performed in the backscattering configuration using a LabRam Horiba HR800 UV spectrometer equipped with an Olympus microscope with a 100× magnification lens. Samples were excited using a laser line at 532 nm. Sample nomenclature is according to the heating rate (HR) and its maximum temperature during selenization. For example, sample selenized at an HR of 2 °C/s and an annealing temperature of 500 °C was named as Se-HR2-T500.

## 3. Results and discussion

### *3.1. Compositional and morphological analysis*

Figures 1(a) to (h) shows the surface morphologies of the selenized samples for different heating rates and maximum annealing temperatures. Comparing these images it can be noted that the surface morphology of samples selenized at low temperatures (400 and 450 °C) consists of very fine grains regardless of the heating rate used. For samples Se-HR1-T400 and Se-HR1-T450 no agglomerations or any other artefacts were observed over the surface, whereas in the case of Se-HR2-T400 and Se-HR2-T450, structures in the form of flakes were observed throughout the surface. EDS point scan over these structures revealed a [Cu]/[Sn] ratio of 1.27

and [Zn]/[Sn] ratio of 0.48. However, the very fine thickness of these structures suggests that the flakes are primarily composed of Sn compounds and the detection of Cu and Zn in EDS are from the underlying layers. With increase in annealing temperature, the sample morphology changes dramatically with the formation of very large grains with well-defined boundaries particularly for Se-HR1-T550, Se-HR2-T500 and Se-HR2-T550. However, comparing samples Se-HR1-T500 and Se-HR1-T550 with Se-HR2-T500 and Se-HR2-T550, it is evident that higher heating rate is beneficial, with the latter set of samples having grains with more than double the size of their former counterparts. Sample Se-HR2-T550 consists mostly of large size grains with an average lateral size of 4.5 μm. This is quite a desirable quality for an absorber material for solar cell. The composition of all the samples measured by EDS is given in table 1. All the samples were basically Zn-poor and Sn-rich. However, the Zn/Sn ratio shows an increase with annealing temperature indicating that more Sn is being lost at higher temperatures. The loss of Sn is more evident in the case of Se-HR2-T550 for which the film composition becomes nearly stoichiometric.

### *3.2. Structural analysis*

Figure 2 shows the XRD pattern of the samples selenized at maximum temperatures of 400, 450, 500 and 550 °C with a heating rate of 1 °C/s. All the samples clearly show the (112) kesterite peak located at a diffraction angle in range between 27–28°; and the (110) reflection of Mo located at around 40.4°. For Se-HR1-T400, the (112) reflections are located at $2\theta = 27.71°$ which is midway between the (112) peak positions of $Cu_2ZnSnSe_4$ ($2\theta = 27.16°$; ICDD card no. 04-010-6295) and $Cu_2ZnSnS_4$ ($2\theta = 28.44°$; ICDD card no. 01-080-8225). This suggests that the sample is composed of a mixed phase viz. CZTSSe. Following the method employed by Salome *et al* [4] the amount of sulfur present in the sample was estimated to be about 43% (see table 2). With the (112) peak being shifted to 27.38° for sample Se-HR1-T450, the estimated sulfur content was only 17.2%. Still lower sulfur concentration was estimated for Se-HR1-T500

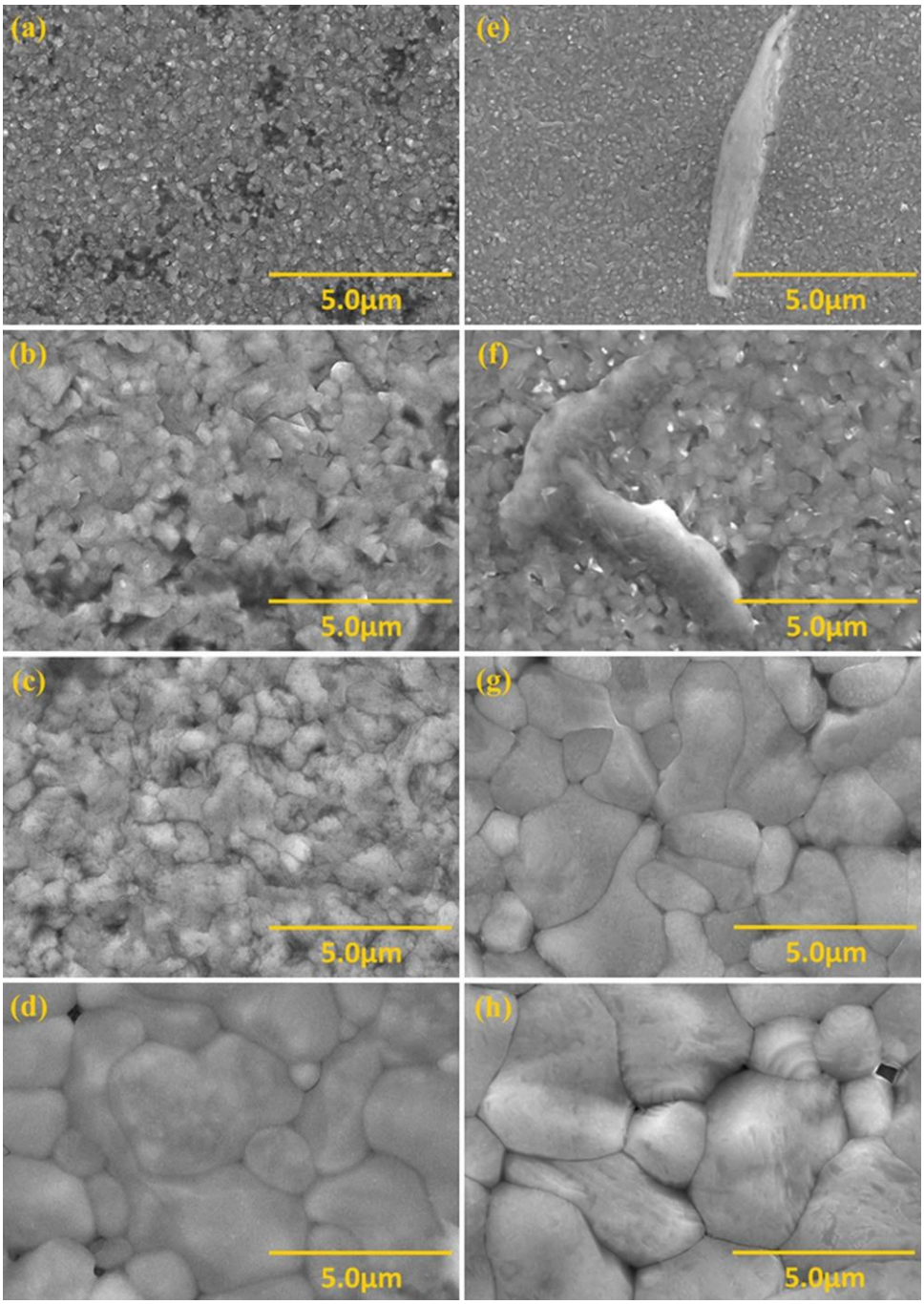


Figure 1. SEM images of samples selenized at different annealing temperatures and with different heating rates. (a) Se-HR1-T400, (b) Se-HR1-T450, (c) Se-HR1-T500, (d) Se-HR1-T550, (e) Se-HR2-T400, (f) Se-HR2-T450, (g) Se-HR2-T500 and (h) Se-HR2-T550.

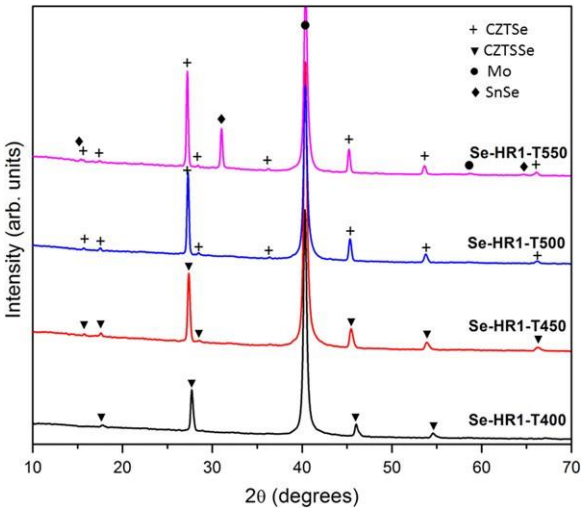


Figure 2. XRD patterns of samples selenized at a heating rate of 1 °C/s.

Table 1. Composition ratio of metallic elements present in the samples.

| Sample | $\frac{[Cu]}{[Zn]+[Sn]}$ | $\frac{[Zn]}{[Sn]}$ | $\frac{[Cu]}{[Zn]}$ | $\frac{[Cu]}{[Sn]}$ |
|---|---|---|---|---|

| | | | | |
|---|---|---|---|---|
| Se-HR1-T400 | 1.11 | 0.51 | 3.32 | 1.68 |
| Se-HR1-T450 | 1.07 | 0.55 | 3.01 | 1.67 |
| Se-HR1-T500 | 1.08 | 0.56 | 3.01 | 1.69 |
| Se-HR1-T550 | 1.17 | 0.68 | 2.89 | 1.96 |
| Se-HR2-T400 | 0.89 | 0.68 | 2.19 | 1.49 |
| Se-HR2-T450 | 1.03 | 0.67 | 2.57 | 1.73 |
| Se-HR2-T500 | 1.09 | 0.76 | 2.52 | 1.91 |
| Se-HR2-T550 | 1.05 | 0.84 | 2.31 | 1.93 |

Table 2. (112) peak position and the estimated sulfur content for the samples.

| Sample name | (112) peak position (degrees) | $\frac{[S]}{([S]+[Se])}$ (%) |
|---|---|---|
| Se-HR1-T400 | 27.71 | 43 |
| Se-HR1-T450 | 27.38 | 17 |
| Se-HR1-T500 | 27.29 | 10 |
| Se-HR1-T550 | 27.22 | 5 |
| Se-HR2-T400 | 27.94 | 61 |
| Se-HR2-T450 | 27.29 | 10 |
| Se-HR2-T500 | 27.16 | 0 |
| Se-HR2-T550 | 27.16 | 0 |

and Se-HR1-T550 since the (112) peak shifts more and more close to that of $Cu_2ZnSnSe_4$ (CZTSe). Nevertheless, allowing for an error margin of ±5% in the calculations, it can be assumed that samples Se-HR1-T500 and Se-HR1-T550 consist of selenide phases only. Except for Se-HR1-T550, no peaks corresponding to secondary phases were observed. Se-HR1-T550, in addition to the characteristic peaks of CZTSe and Mo, exhibits a strong peak at 31.03°. The

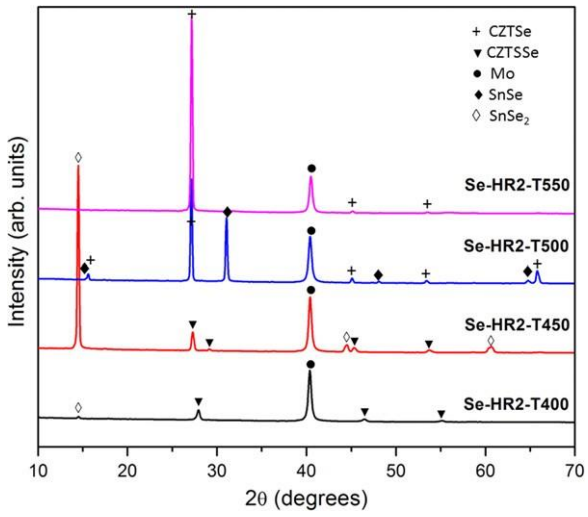


Figure 3. XRD patterns of samples selenized at a heating rate of 2 °C/s.

reason for the presence of this peak only in this sample is unclear. However, it may be attributed

to the α-SnSe phase with the orthorhombic structure (ICDD card no. 04-006-8169). Meanwhile, signatures of other phases such as $Cu_2SnSe_3$ (CTSe), $Cu_2SnS_3$ (CTS) or $Cu_2Sn(S,Se)_3$ (CTSSe) which are expected to be present due to the Sn excess in these samples could not be confirmed from XRD.

As seen from the SEM images, the heating rate of 2 °C/s has a dramatic influence on the morphology of the samples. This is also evident in the XRD pattern of the samples (see figure 3). Sample Se-HR2-T400 shows the characteristic peaks of CZTSSe with the dominant peak at 27.94° and the (110) peak of Mo at 40.4°. Apart from these peaks, a small peak at 14.53° is observed in the diffraction pattern which can be due to hexagonal $SnSe_2$ phase (ICDD card no. 01-089-2939) present in the sample. Recalling from the SEM analysis that Se-HR2-T400 and Se-HR2-T450 consists of flake-like formations over the surface which are presumed to be related to some phases of Sn, it is probable that the reflections at 14.53° are from these flakes themselves. For Se-HR2-T450, this peak becomes very intense, indicating the formation of highly crystalline $SnSe_2$ phases. The (112) kesterite peak for this sample is shifted to 27.29°, indicating a considerable loss of sulfur at this temperature. At 500 °C, the $SnSe_2$ phases disappear completely and only the characteristic peaks of CZTSe, Mo and α-SnSe are observed. The sample becomes completely selenized at this temperature without any trace of sulfur remaining. At 550 °C, the α-SnSe phase also vanishes and the sample consists of only the CZTSe phase.

Raman spectra of the samples Se-HR1-T400, Se-HR1-T450, Se-HR1-T500 and Se-HR1-T550 are presented in figure 4. All the spectra except for Se-HR1-T400 are similar with major peaks at about 173, 195 and 235 $cm^{-1}$ and a faint peak at 330 $cm^{-1}$. Peaks at 173, 195, 235 $cm^{-1}$ are characteristic of the CZTSe phase present in the sample [16, 17] while the peak at 330 $cm^{-1}$ is assigned to the $Cu_2ZnSnS_4$ (CZTS) phase [16, 17]. For Se-HR1-T400, the Raman spectra consists of a very broad peak in the range 150 to 250 $cm^{-1}$, a close inspection of which reveals several overlapping peaks at about 173, 180, 195, 209, 219 and 235 $cm^{-1}$. Also, a peak at 330 $cm^{-1}$ with a shoulder at 350 $cm^{-1}$ is observed for this sample. These peaks can be assigned to CZTSe (173, 195 and 235 $cm^{-1}$), CZTSSe (209, 330 and 350 $cm^{-1}$) [16], CTSe (180 and

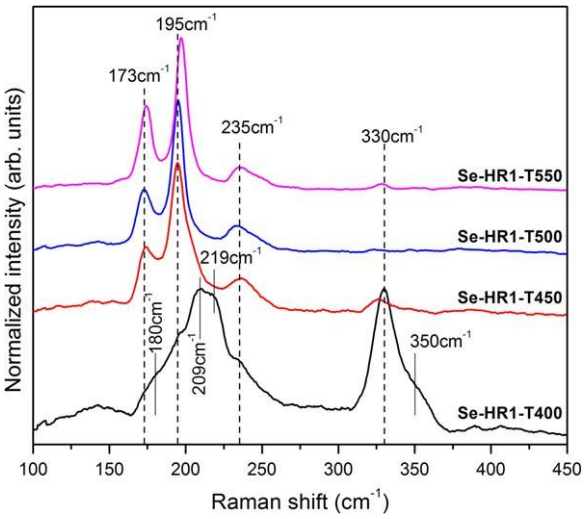


Figure 4. Raman spectra of samples Se-HR1-T400, Se-HR1-T450, Se-HR1-T500 and Se-HR1-T550.

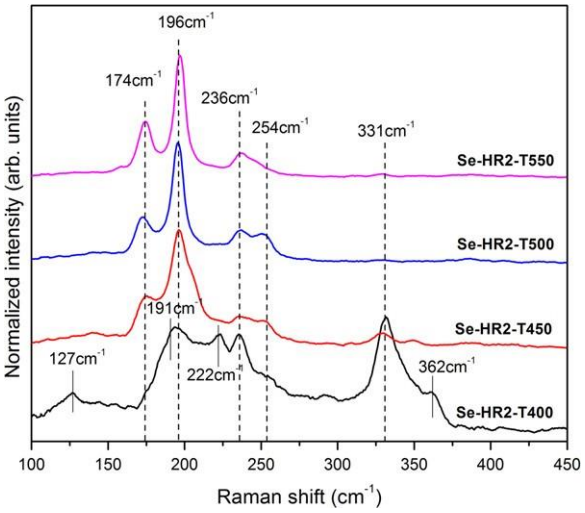


Figure 5. Raman spectra of samples Se-HR2-T400, Se-HR2-T450, Se-HR2-T500 and Se-HR2-T550.

235 $cm^{-1}$) [18] and SnS (219 $cm^{-1}$) [19] phases present in the surface layers of the sample. However, no information about the CTSe and SnS phases was obtained from the XRD analysis of this sample.

Raman spectra of samples annealed at heating rate of 2 °C/s (figure 5) also shows a similar trend as compared to the samples prepared at heating rate of 1 °C/s. However, compared to the spectrum of Se-HR1-T400 no peaks corresponding to CTSe and SnS were observed for Se-HR2-T400 whereas additional peaks at 127, 191, 254 and 362 $cm^{-1}$ were detected. The peak at 127 and 191 $cm^{-1}$ may be assigned to $Sn(S_{0.2}Se_{0.8})_2$ [20, 21] and the one at 254 $cm^{-1}$ could be

due to amorphous selenium as indicated in earlier reports [21]. The peak at 362 $cm^{-1}$ is associated with CZTS [16, 17], the fact being it is shifted to lower wavenumbers just like the

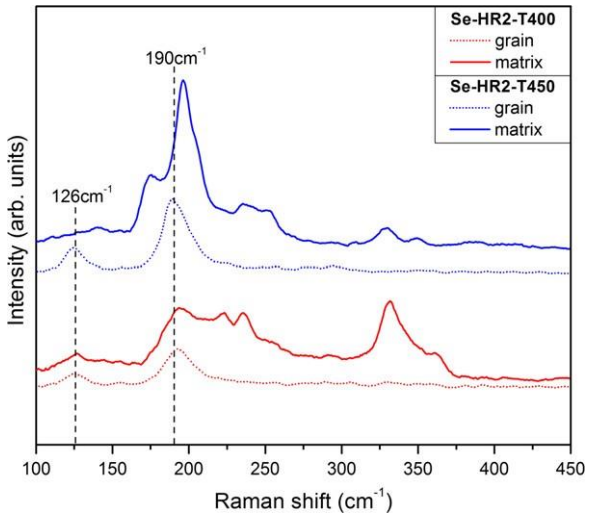


Figure 6. Raman spectra of Se-HR2-T400 and Se-HR2-T450. Solid and dotted lines represent the spectra recorded from the film matrix and grain (flake-like structure), respectively.

peak at 331 $cm^{-1}$ due to the replacement of sulfur atoms by selenium within the CZTS lattice [16].

Again, Raman analysis was employed to have conclusive information about the exact nature of the flake-like growth over the surface of samples Se-HR2-T400 and Se-HR2-T450. Figure 6 gives a comparison between spectra recorded from the grains (flakes) and from the area devoid of these features. Raman measurements clearly show two well defined peaks at 126 and 190 $cm^{-1}$ for these grains which may be assigned to $Sn(S_{0.2}Se_{0.8})_2$ phases as mentioned

previously. Looking into the spectra recorded from the film matrix, it may be noted that these mixed phases are present only in Se-HR2-T400. Hence, it is reasonable to assume that at 450 °C almost all of the excess Sn in the film matrix has segregated over the surface to form $Sn(S_{0.2}Se_{0.8})_2$ grains.

## 4. Conclusions

Rapid thermal processing was employed to prepare kesterite CZTSSe thin films from stacked precursor layers. The effect of selenization temperature and heating rate on the compositional, structural and morphological properties of the films was investigated. Results suggest that high heating rate and high annealing temperature is necessary to obtain films with good crystallinity and to avoid the formation of secondary phases. However, it appears that the amount of sulfur present in the precursors is not sufficient to produce a CZTSSe phase at these temperatures and that additional supply of sulfur during annealing is required. Higher sulfur content in the film was observed only at low selenization temperatures. It is also worth mentioning that sulfur in the precursor gets easily replaced by selenium with increase in temperature. Films prepared at the selenization temperature of 550 °C and heating rate of 2 °C/s were found to be the best in terms of composition, morphology and structural properties. The films prepared in those conditions were composed of very large grains with average lateral size of about 4.5 μm with a composition that is nearly stoichiometric. It was concluded from XRD and Raman analysis that the film was devoid of any secondary phases.

## Acknowledgments

M R Rajesh Menon acknowledges the financial support provided through the project 'Harvesting the energy of the Sun for a sustainable future', Projeto 07/ST24/FEDER/002032 (CENTRO). Samaneh Ranjbar thanks the financial support of the Portuguese Science and Technology Foundation (FCT) through PhD grant SFRH/BD/78409/2011. The authors also wish to acknowledge FCT for supporting this work through the grants PTDC/CTM-MET/113486/2009, PESTC/CTM/LA0025/2011 and RECI/FIS-NAN/0183/2012.

## References


[1] Ki W and Hillhouse H W 2011 Earth-abundant element photovoltaics directly from soluble precursors with high yield using a non-toxic solvent *Adv. Energy Mater.* **1** 732–5

[2] Lechner R, Jost S, Palm J, Gowtham M, Sorin F, Louis B, Yoo H, Wibowo R A and Hock R 2013 $Cu_2ZnSn(S,Se)_4$ solar cells processed by rapid thermal processing of stacked elemental layer precursors *Thin Solid Films* **535** 5–9

[3] Wibowo R A, Yoo H, Hölzing A, Lechner R, Jost S, Palm J, Gowtham M, Louis B and Hock R 2013 A study of kesterite $Cu_2ZnSn(Se,S)_4$ formation from sputtered Cu–Zn–Sn metal precursors by rapid thermal processing sulfo-selenization of the metal thin films *Thin Solid Films* **535** 57–61

[4] Salome P M P, Malaquias J, Fernandes P A, Ferreira M S, da Cunha A F, Leitao J P, Gonzalez J C and Matinaga F M 2012 Growth and characterization of $Cu_2ZnSn(S,Se)_4$ thin films for solar cells *Sol. Energy Mater. Sol. Cells* **101** 147–53

[5] Grenet L, Bernardi S, Kohen D, Lepoittevin C, Noel S, Karst N, Brioude A, Perraud S and Mariette H 2012 $Cu_2ZnSn(S_{1-x}Se_x)_4$ based solar cell produced by selenization of vacuum deposited precursors *Sol. Energy Mater. Sol. Cells* **101** 11–4

[6] Ge J, Zuo S, Jiang J, Ma J, Yang L, Yang P and Chu J 2012 Investigation of Se supply for the growth of $Cu_2ZnSn(S_xSe_{1-x})_4$ ($x \approx 0.02$–$0.05$) thin films for photovoltaics *Appl. Surf. Sci.* **258** 7844–8

[7] Guo Q, Ford G M, Yang W-C, Walker B C, Stach E A, Hillhouse H W and Agrawal R 2010 Fabrication of 7.2% efficient CZTSSe solar cells using CZTS nanocrystals *J. Am. Chem. Soc.* **132** 17384–6

[8] Cao Y *et al* 2012 High efficiency solution processed $Cu_2ZnSn(S,Se)_4$ thin film solar cells prepared from binary and ternary nanoparticles *J. Am. Chem. Soc.* **134** 15644–7

[9] Wang W, Winkler M T, Gunawan O, Gokmen T, Todorov T K, Zhu Y and Mitzi D B 2014 Device characteristics of CZTSSe thin film solar cells with 12.6% efficiency *Adv. Energy Mater.* **4** 1–5

[10] Salomé P M P, Fernandes P A and da Cunha A F 2009 Morphological and structural characterization of $Cu_2ZnSnSe_4$ thin films grown by selenization of elemental precursor layers *Thin Solid Films* **517** 2531–4

[11] Fella C M, Uhl A R, Romanyuk Y E and Tiwari A N 2012 $Cu_2ZnSnSe_4$ absorbers processed from solution deposited metal salt precursors under different selenization conditions *Phys. Status Solidi* **209** 1043–8

[12] Scragg J J, Dale P J, Colombara D and Peter L M 2012 Thermodynamic aspects of the synthesis of thin film materials for solar cells *Chem. Phys. Chem.* **13** 3035–46

[13] Scragg J J, Ericson T, Kubart T, Edoff M and Platzer-Björkman K C 2011 Chemical insights into the instability of $Cu_2ZnSnS_4$ films during annealing *Chem. Mater.* **23** 4625–33

[14] Redinger A, Berg D M, Dale P J and Siebentritt S 2011 The consequences of kesterite equilibria for efficient solar cells *J. Am. Chem. Soc.* **133** 3320–3

[15] Hartt M J and Evans A G R 1988 Rapid thermal processing in semiconductor technology *Semicond. Sci. Technol.* **3** 421–36

[16] Grossberg M, Krustok J, Raudoja J, Timmo K, Altosaar M and Raadik T 2011 Photoluminescence and Raman study of $Cu_2ZnSn(Se_xS_{1-x})_4$ monograins for photovoltaic applications *Thin Solid Films* **519** 7403–6

[17] Khare A, Himmetoglu B, Johnson M, Norris D J, Cococcioni M and Aydil E S 2012 Calculation of the lattice dynamics and Raman spectra of copper zinc tin chalcogenides and comparison to experiments *J. Appl. Phys.* **111** 083707

[18] Altosaar M, Raudoja J, Timmo K, Danilson M, Grossberg M, Krustok J and Mellikov E 2008 $Cu_2Zn_{1-x}Cd_xSn(Se_{1-y}S_y)_4$ solid solutions as absorber materials for solar cells *Phys. Status Solidi* **205** 167–70

[19] Chandrasekhar H R, Humphreys R G, Zwick U and Cardona M 1977 Infrared and Raman spectra of the IV–VI compounds SnS and SnSe *Phys. Rev.* B **15** 2177

[20] Hadjiev V G, De D, Peng H B, Manongdo J and Guloy A M 2013 Phonon probe of local strains in $SnS_xSe_{2-x}$ mixed crystals *Phys. Rev.* B **87** 104302

[21] Fernandes P A, Sousa M G, Salomé P M P, Leitão J P and da Cunha A F 2013 Thermodynamic pathway for the formation of SnSe and $SnSe_2$ polycrystalline thin films by selenization of metal precursors *CrystEngComm* **15** 10278–86